Polymer 50 (2009) 4372–4377

Contents lists available at ScienceDirect

Polymer

journal homepage: www.elsevier.com/locate/polymer

The role of acidic *m*-cresol in polyaniline doped by camphorsulfonic acid

Ki-Ho Lee [a], Bong Jun Park [b], Dong Hyun Song [b], In-Joo Chin [b], Hyoung Jin Choi [b,*]

[a] School of Computational Sciences, Korea Institute for Advanced Study, Seoul 130-722, Republic of Korea
[b] Department of Polymer Science and Engineering, Inha University, Incheon 402-751, Republic of Korea

ARTICLE INFO

Article history:
Received 7 April 2009
Received in revised form
4 July 2009
Accepted 8 July 2009
Available online 22 July 2009

Keywords:
Polyaniline
Conducting polymer
Camphorsulfonic acid

ABSTRACT

Camphorsulfonic acid (CSA) and *m*-cresol are known to be one of the most effective pairs of dopant and solvent for polyaniline (PANI) doping, respectively. Although the concept of secondary dopant that modifies the conformation of PANI has been a major description for the role of *m*-cresol, the acidity of *m*-cresol also has been suggested as one of the crucial factors enhancing electron mobility of PANI. A *m*-cresol molecule is small enough to diffuse into PANI cluster, and it has ability to exchange a proton with a camphorsulfonate ion and PANI, while CSA is relatively big to stay in PANI crystalline region. Experiments and semiempirical quantum mechanics calculations were used in this study to investigate the role of acidic *m*-cresol in PANI. When 3-methylphenolate ions stay in PANI cluster, energy band gap is predicted to decrease for polaronic and bipolaronic structures, while undissociated *m*-cresol does not work for doping.

1. Introduction

Since conjugated polymers demonstrate versatile electronic properties, they have been suggested for or applied to various electronic devices such as polymer light emitting diodes [1], batteries [2], memory devices [3], electro-magnetic interference (EMI) shielding [4], and electrorheology [5–7]. Especially, polyaniline (PANI) examined in this study is one of the most favorable conjugated polymers for its chemical stability, yield and producing cost along with its various composite systems [8–10]. As long as PANI is in the form of an undoped base, it shows the properties of an organic semiconductor. The conducting behavior of PANI is able to be attained by the addition of a dopant, and its electric conductivity of the PANI salt depends on the type of dopant [11–13]. Two different doping processes, *p*-type doping and protonic acid doping, have been used to manufacture conductive PANI. When the leucoemeraldine base (LEB) of PANI is doped with an oxidizing agent such as iodine, its electric conduction can be acquired due to remarkable enhancement in electric conductivity [13]. Various protonic acids can also help PANI emeraldine base (EB) blast the transport of electrons in another way [14]. It is hard to compare the exclusive effects of different acids on the conductivities of PANI emeraldine salt (ES), because they also depend on solvent that is paired with the chosen acid. When HCl is used for the dopant in the form of aqueous solution, the electric conductivity of the PANI salt goes up to 5 S/cm unless stretching or any chemical modification [15]. Although water cannot make PANI soluble for difference in their polarities, it is a vital medium for the oxidative polymerization of aniline working with HCl that is not only a dopant but also an agent for the electrolysis of ammonium persulfate. Camphorsulfonic acid (CSA) is an another protonic acid for PANI EB doping. Recently, electric conductivity higher than 10^3 S/cm was obtained by Lee et al. [16] using a dispersion polymerization and CSA doping in *m*-cresol. It is well known that more effective electron transport can be achieved when the *m*-cresol is used for a solvent than when *N*-methyl-2-pyrrolidinone (NMP) or chloroform is added as an alternative solvent [17]. Therefore, it is obvious that an appropriate combination of dopant and solvent enhances the transport of electrons for some reasons. This study is primarily concerned with how both dopant and solvent work cooperatively for the electron transfer.

One of the most remarkable studies about the role of *m*-cresol in the CSA doping of PANI has been carried out by MacDiarmid and Epstein [18]. They have presented many experimental observations to support their "secondary dopant" concept that *m*-cresol and many other phenol derivatives participate in expanding PANI molecules which are initially of coil-like conformations, and results in changing the crystalline structure of PANI ES. Thereby, the relationship between primary and secondary dopants have attracted many research groups' attention: for example, Jayakannan et al. experimentally studied special types of dopants, which have both sulfonic acid and phenolate in a single molecule, and found that a methyl group on the phenolate side changes the electric properties of PANI [19]. Further, the concept of secondary dopant has

* Corresponding author. Tel.: +82 328607486; fax: +82 328655178.
E-mail address: hjchoi@inha.ac.kr (H.J. Choi).

0032-3861/$ – see front matter © 2009 Elsevier Ltd. All rights reserved.
doi:10.1016/j.polymer.2009.07.009

been consolidated with more experimental results and an additional idea that the doping effectiveness of CSA depends on the acidic dissociation of a secondary dopant [20]. In this study experimental approaches have been executed to investigate the role of acidic *m*-cresol for CSA doping of PANI.

PANI bases and salts have been studied for the molecular conformations and the energy levels by various types of computations for more than 20 years. Density functional theory (DFT) [21,22] and Hartree–Fock (HF) [23] calculations have provided interesting and reliable predictions on the first level of quantum mechanics for PANI. However, those quantum mechanical computations are still very expensive even for an oligomeric molecule unless periodic boundary conditions are adopted, while semiempirical methods make it possible to deal with a much bigger system for shorter calculation time. Modified neglect of differential overlap (MNDO) semiempirical methods were simply used to optimize the dimeric and tetrameric structures of PANI bases and salts in the 1980s [24,25]. Later Austin Model 1 (AM1) semiempirical studies have been carried out for more complicated systems such as the conformations and molecular orbitals of longer PANI chains [21,26], and the supramolecular structures of PANI with dopants and with solvents [27–29]. Recently, we reported conformations of PANI bases studied via semiempirical methods [30]. In this study we also computationally examine the structures that consist of PANI octamers, CSA, benzene and *m*-cresol with AM1 and Parametric Model number 3 (PM3) semiempirical methods in addition to the experimental investigation.

2. Experimental and computational details

2.1. Experimental methods

While 1.0 M HCl aqueous solution was being agitated at 0 °C, aniline monomer was slowly dropped into the solution for sustaining of stable suspension. Initiator solution, which was made of ammonium persulfate (APS) and HCl aqueous solution (pH ~ 0.07), was dropped to the dispersion of aniline for 3 h [31]. After this primary polymerization, the temperature of the PANI-dispersed liquid was raised up and maintained at 25 °C for 24 h to proceed the secondary polymerization of residual monomers. Because the PANI produced from this procedure was already in the state of self-doped PANI by HCl, dedoped PANI base should be prepared by dedoping the self-doped PANI with NaOH. A centrifuge made the suspended PANI base or salt be precipitated in the dispersed mixture, and then the precipitate was washed by distilled water before it was dried. PANI powders were with *m*-cresol and 0.1 M CSA *m*-cresol solution for 24 h, and then were dried again at 50 °C for final samples. Note that emulsion polymerization of PANI has been also widely tested [32]. The electrical conductivities of powder types of the PANI bases and salt were measured by the four-probe method (resistivity meters, MCP-T610 and MCP-HT450, Mitsubishi Chemical Co., Japan).

2.2. Computational details

A geometrical structure of PANI EB octamer was built, and then it was computationally optimized with MM3 molecular mechanics force field [33] in Tinker package. This package generated various conformations using a program module, which is called Scan, by changing five times per each torsion angles in the molecules, and optimized 982 molecular geometries again with MM3 force field. Then AM1 semiempirical electronic structure method in GAMESS package [34] was used to optimize the individual structures to obtain more approved structures. The longest conformation of PANI EB was chosen to construct packed structures of nine octamers of the same conformation, and the structures with CSA or *m*-cresol were reoptimized. This procedure is primarily influenced by van der Waals interaction between composed chain molecules. The semiempirical self-consistency fields of restricted Hartree–Fock (RHF) and restricted open shell Hartree–Fock (ROHF) were used for bipolaronic and polaronic structures, respectively. Gaps between the highest occupied molecular orbital (HOMO) and the lowest unoccupied molecular orbital (LUMO) for bipolaronic structures or between singly occupied molecular orbital (SOMO) and LUMO levels for polaronic structures were calculated for doped structures. Thermodynamic properties of CSA and *m*-cresol were also examined computationally at the levels of semiempirical AM1 and of *ab initio* RHF with basis set 6-31++G(d,p).

3. Results and discussion

It is well known that HCl-doped PANI salt consists of both crystalline domain and amorphous region while dedoped PANI base produced from the salt is wholly amorphous. The crystalline domain size of the ES is about 50 Å and the crystallinity of the ES is 50% at most [35,36]. If PANI films are cast from NMP or *m*-cresol solutions, about 15 wt% of the solvents still remain in the films after evaporation [15]. Therefore, the bulk state of PANI inherently has free volume that can trap small molecules. In order to examine the diffusion of *m*-cresol in PANI, several samples were prepared for thermogravimetric analysis (TGA). Cresol-swollen PANI ES (a) of Fig. 1 is a sample of HCl-doped ES that was mixed with *m*-cresol for 24 h under agitation, and cresol-swollen PANI ES (b) is one that was just immersed in *m*-cresol without forced convection. Both cresol-swollen samples were dried in vacuum oven at 50 °C for 100 h to produce solid films. In Fig. 1 the TGA curves of cresol-swollen PANI ES samples show abrupt decay in their weight after 100 °C, while the weight of HCl-doped ES decreases slowly until 350 °C. These changes indicate that *m*-cresol diffuses easily into PANI crystal and it builds strong interaction with PANI chains. When *m*-cresol molecules once migrate into emeraldine solid, delocalized π bonds on the phenyl group of *m*-cresol induce π–π stacking interaction with the phenyl groups in the backbone of PANI, and its hydroxyl group builds strong hydrogen bonding with amine group.

Generally, the state of PANI after doping process used to be explained with its crystalline structure. Fig. 2 demonstrates the X-ray diffraction pattern of both HCl-doped PANI and CSA-doped PANI/*m*-cresol. The spectrum of CSA-doped PANI/*m*-cresol shows strikingly high peaks at 16.1° and 19.5° which correspond the *d*-spacing of 5.5 Å and 4.5 Å, while that of HCl-doped ES shows blunt

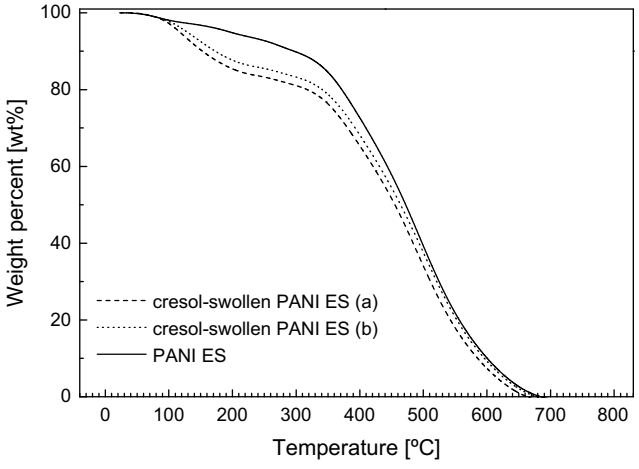

Fig. 1. Thermogravimetric analysis of PANI samples.

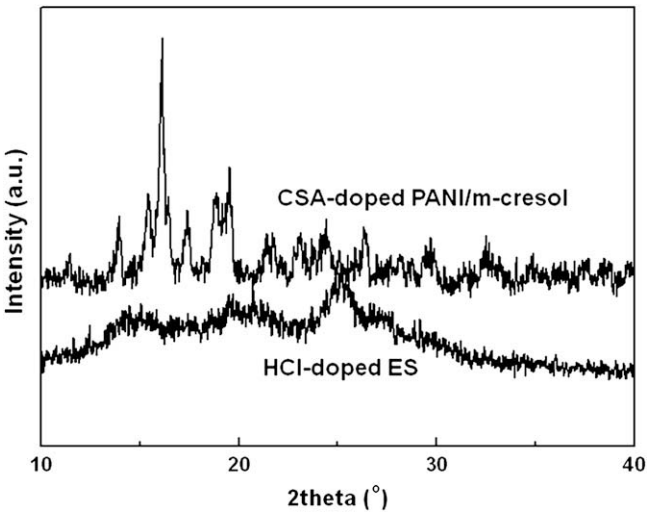

Fig. 2. XRD pattern of HCl-doped PANI and CSA-doped PANI/*m*-cresol samples.

peaks at 2θ's of 14.8°, 19.8° and 25.4°. That more than one peak of low height spread around 25° for the CSA-doped PANI/*m*-cresol system is considered to be caused by the existence of residual *m*-cresol in the interstitial sites of PANI crystalline regions, because something bigger than Cl^- ion may disturb the fine alignment of the (110) crystal plane corresponding to the 2θ at 25° for ES-I.

Experimental electric conductivities of PANI containing residual *m*-cresol are given in Table 1. The extent of increase in electric conductivity is about 27% for HCl self-doped PANI ES when it is treated only by *m*-cresol, and 46% of the electric conductivity increases by the addition of CSA to self-doped ES in an aqueous medium, which shows a little change made by CSA only. Since the electric conductivity of HCl-doped ES/CSA/*m*-cresol system is much higher than that of HCl-doped ES/*m*-cresol system, it can be concluded that *m*-cresol as the secondary dopant obviously works better only with CSA, while the sole effect of *m*-cresol is less remarkable. In addition, when dedoped EB is once dissolved in *m*-cresol, EB/*m*-cresol (I) with residual *m*-cresol has higher conductivity than vacuum-dried EB/*m*-cresol (II) which is expected to include lower content of *m*-cresol.

Computational chemistry methods can provide information about the activity of CSA and *m*-cresol in PANI. HCl is small enough to diffuse into PANI semicrystal and to stay in the interstitial positions working as a dopant, but a CSA molecule is expected to have lower diffusivity for its bigger size than HCl. The molecular shape of CSA obtained from AM1 optimization is anisotropic with the approximate dimensions of 8.2 Å × 6.1 Å × 5.6 Å assuming that the atomic sizes of all atoms are about 1 Å. It was reported that the atomic diffusion of a solute atom is allowed to commence from an interstitial site to another only if the ratio of the radius of the solute to that of host atom should be below 0.59, and the diffusion coefficients decrease with the ratio [37].

Table 1
The electric conductivities of HCl-doped PANI ES, CSA-doped PANI ES and dedoped PANI EB.

PANI	Conductivity [S/cm]
HCl-doped ES	4.374×10^{-2}
HCl-doped ES/*m*-cresol	5.561×10^{-2}
HCl-doped ES/CSA/water	6.492×10^{-2}
HCl-doped ES/CSA/*m*-cresol	6.4
EB/*m*-cresol (I)	10^{-3} to 10^{-4}
EB/*m*-cresol (II)	10^{-11}
CSA-doped/*m*-cresol	60

Interstitial diffusion of CSA molecules between two nearest interstitial positions is also expected to depend on the lattice constant of the crystalline structure. Therefore, the lattice constant or interchain distance of PANI cluster should be longer than 9.5 Å at least for the shortest side of CSA to allow the diffusion of the dopant. According to the study of Pouget et al. the lattice constants of PANI are 4.3 Å × 5.9 Å for ES-I, 7.1 Å × 7.9 Å for ES-II, and 7.7 Å × 5.8 Å for EB-II [38]. Consequently, it is predicted that CSA molecules cannot diffuse into a crystalline domain of PANI, or that they inhibit the formation of crystalline domain during recrystallization. If this inference is pertinent, doping of PANI with CSA is expected to happen mostly in the amorphous region or on the surface of crystalline domain. This prediction can be confirmed by AM1 method. The initial structure of PANI cluster was built by packing nine PANI chains of the same conformation, which is the longest EB octamer out of 982 different conformations, in 3 by 3 manners, and then was optimized by AM1 calculations. This optimized structure of the EB cluster is not identical with any crystalline structure proposed by Pouget et al., however it is enough to learn the deformation of PANI cluster. Although why we could not build the geometries corresponding to the proposed structures is probably an interesting issue to discuss, but it is intended to be out of the concern in this study. One chain at a corner was translated aside by few angstroms, and deprotonated camphorsulfonate ions were inserted between the chains, and the whole structure of the cluster was optimized. Fig. 3 shows a front view and a side view of the optimized structure of packed PANI octamers, in which two camphorsulfonate ions are inserted. The numbers labeled in Fig. 3a distinguish PANI chains, and those in Fig. 3b identify the sites or the units of anilines along each chain. Two camphorsulfonate ions are surrounded by chains 1, 2, 7 and 8 in Fig. 3a. The sites of the central

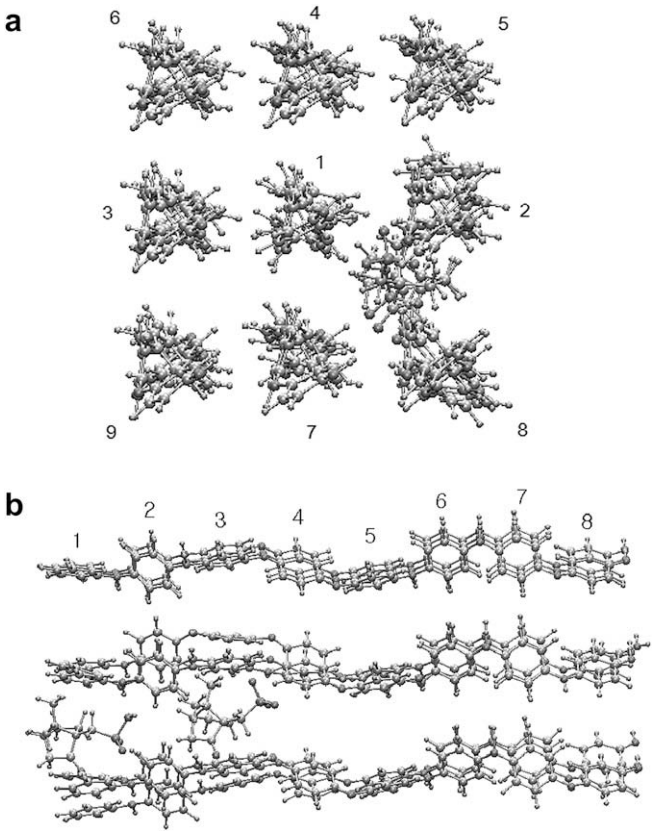

Fig. 3. An optimized structure of PANI octamers intercalated into by camphorsulfonate ions. (a) Front and (b) side views.

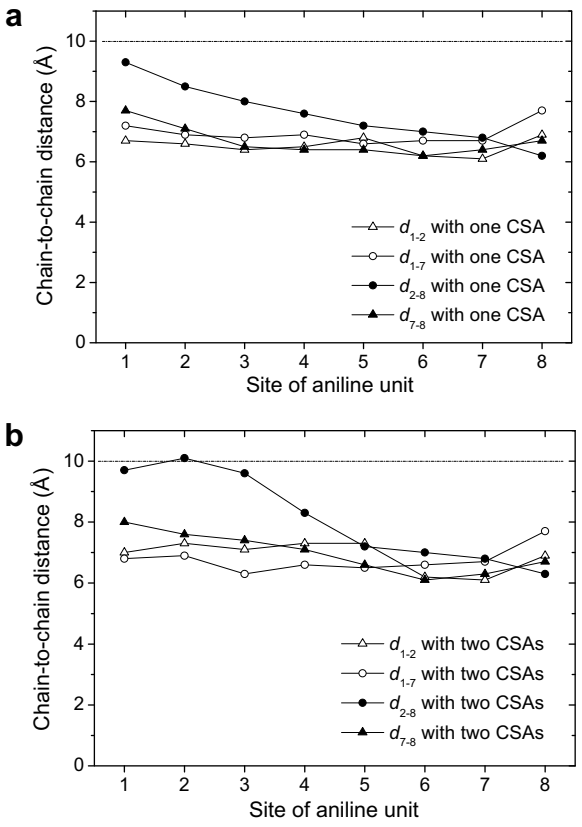

Fig. 4. Chain-to-chain distance of PANI octamers in which camphorsulfonate ions intrude. (a) One ion is laid at the site 1, and (b) two ions are laid at sites 1 and 3.

PANI octamer (chain 1) with which camphorsulfonate ions are associated with are 1 and 3 in Fig. 3b.

According to Fig. 4, which shows the chain-to-chain distances between the identical sites on two PANI chains after one or two camphorsulfonate ions are inserted, the distance between chains 1 and 8 (d_{2-8}) is larger than the distance between chains 1 and 7 (d_{1-7}) by more than 2 Å at site 1. These two distances are expected to be similar with each other unless camphorsulfonate ions are inserted. The distance d_{1-2} at the sites 1 and 3 is as long as 9.5 Å that is previously proposed for the diffusion of CSA. These local displacements of PANI chains by the insertion of CSA obstruct PANI chains to align in regular pattern. AM1 calculations give 2.7 and 3.8 eV of the SOMO–LUMO gaps for one and two sulfonate ions, respectively, in polaronic configuration of PANI. Since the calculated HOMO–LUMO gap is 6.0 eV for the structure of the EB, it is found that

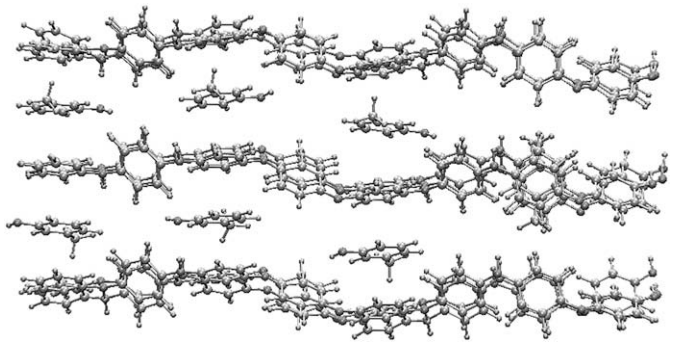

Fig. 5. An optimized structure of packed PANI octamers in which eight *m*-cresol molecules are intercalated.

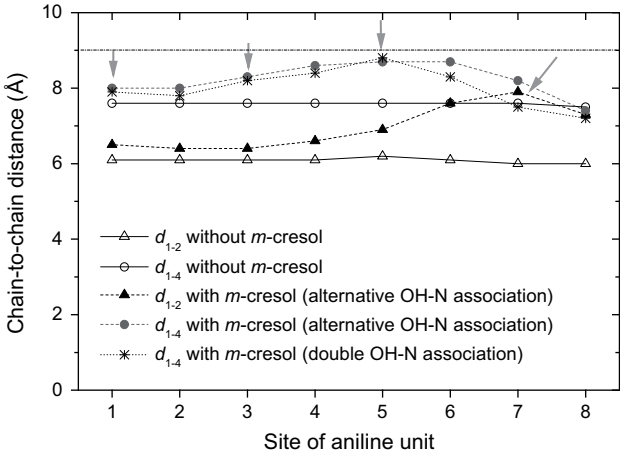

Fig. 6. Chain-to-chain distances of the packed PANI structure in which eight *m*-cresol molecules are intercalated.

camphorsulfonate ions contribute to the enhancement of electric conduction for doping effect regardless of PANI structure.

The effect of *m*-cresol on a structure of PANI EB cluster has been studied with AM1 optimization when eight *m*-cresol molecules are inserted into interstitial positions along the central PANI molecule as shown in Fig. 5. A hydroxyl group of *m*-cresol and an amine (or imine) group of aniline are associated with alternative manner while every two *m*-cresol molecules are faced to same aniline sites 1, 3, 5 and 7 of the central PANI chain 1. Double OH–N association implies that an amine or an imine group of the central EB molecule is simultaneously associated with two OH groups of *m*-cresols facing to the same aniline site. The deformation of a PANI cluster due to the insertion of *m*-cresol molecules was examined with the change in the distance between PANI chains in Fig. 6. Downward arrows indicate both the aniline sites *m*-cresol molecules associated with and PANI chains sandwiching the *m*-cresol. *m*-Cresols at sites 1, 3 and 5 are laid between chains 1 and 4 while another at site 7 is between chains 1 and 2. d_{1-4} increases by less than 1 Å due to the insertion of *m*-cresol at sites 1 and 3 compared with that in the optimized structure without *m*-cresol, however d_{1-4} at site 5 and d_{1-4} at site 7 increase by more than 1 Å. Therefore, it is found that the diffusion of *m*-cresol into PANI cluster can be achieved with much less deformation of PANI structure than that of CSA depending on the states of interstitial position.

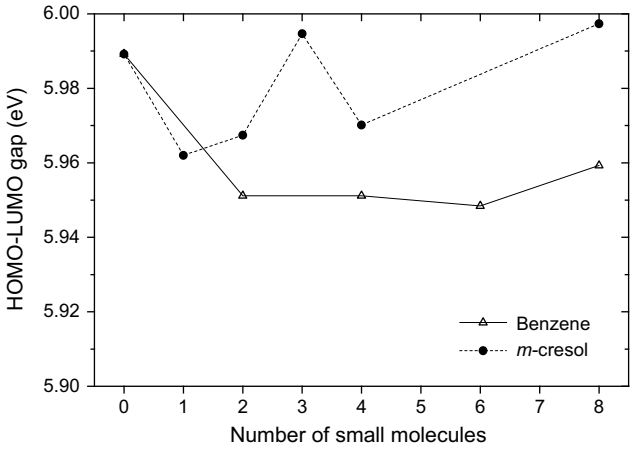

Fig. 7. HOMO–LUMO gap of packed PANI octamers with benzene or undissociated *m*-cresol.

When benzene or undissociated *m*-cresol molecules are intercalated into PANI, the alteration in molecular orbitals of PANI cluster can be imagined, because the conjugated π orbitals in *m*-cresol can form π–π stacking interaction with benzenoid rings of PANI. According to Fig. 7, however, unnoticeable change in the HOMO–LUMO gap from AM1 calculations is predicted due to the addition of benzene rings by the same manner in Fig. 4. Undissociated *m*-cresol is also predicted to affect merely the electrical properties of PANI. Therefore, the π–π stacking of PANI with a delocalized phenyl group in a small molecule barely affects the conductive properties of PANI EB.

Since *m*-cresol assists the hydrogen trading between EB and CSA as referred in the Introduction, the restriction of CSA doping can be supported by the acidic dissociation of *m*-cresol. CSA is dissociated into a proton H^+ and a camphorsulfonate ion as shown in reaction formula (1).

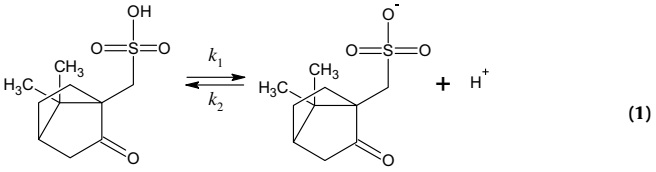

(1)

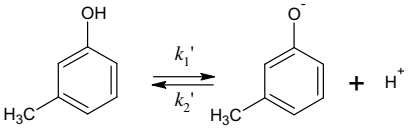

(2)

pK_a of CSA is known to be −2 in water [39], and *m*-cresol is also dissociated as described in reaction formula (2) with pK_a = 10, while pK_a of water is 14 [40]. Because bulk CSA is of solid state at room temperature, it is hard to compare appropriately its acidity with that of *m*-cresol. Standard Gibbs free energies for the reaction formulas (1) and (2) were evaluated with AM1 semiempirical methods and with *ab initio* calculations as listed in Table 2. Since $\Delta G^\circ = -RT \ln K_a$ where *R* is gas constant, *T* is temperature and K_a is acid dissociation constant, K_a can be predicted from ΔG°. If reaction formulas (1) and (2) are combined, the exchange of a proton between CSA and *m*-cresol is represented as following formula (3).

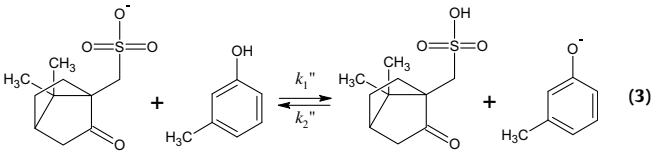

(3)

When equilibrium constant *K* for reaction formula (3) is defined as k_1''/k_2'', calculated *K*s are calculated as 0.777 from AM1 calculation, 20.3 from RHF/6-31++G(d,p), and 16.2 from RHF/6-31++G(d,p) scaled by 0.89 at 298.15 K. Because it is expected that the deprotonation of CSA is more prevailing than the dissociation of *m*-cresol into 3-methylphenolate, *K* from AM1 calculation is most trustworthy. In any case 3-methylphenolate can be expected to assist proton exchanging between CSA and PANI EB. Since the free energy of solvation is not included in these calculations, the equilibrium dissociation of CSA and *m*-cresol needs to be examined by more convinced way such as pH measurement. pH of *m*-cresol is about 4.3, thus *m*-cresol is obviously one of the weak acids. However, it was found that small amount of CSA could drop pH of *m*-cresol according to the results that pH is −0.2 for 1.0×10^{-4} M and 2.1 for 0.5×10^{-4} M CSA/*m*-cresol solution. Compared with measurements that pH of 0.1 M CSA aqueous solution is about 1.13 and that of 0.1 M HCl aqueous solution is about 0.7, the protonation of CSA/*m*-cresol solution must be a synergetic process. An idea suggested for the synergetic phenomenon can be that electronegative oxygens of one sulfonic acid molecule can share protons with more than one *m*-cresol molecule, thus more protons can get stable in the solution than HCl aqueous solution. The idea about proton-sharing sulfonic acid has been adopted to the study of fuel cell membranes [41].

Table 2
Gibbs free energies of dopants in kJ/mol at 298.15 K.

	d-CSA			*m*-Cresol		
	G_{HA}	G_A^+	ΔG°	G_{HA}	G_A^+	ΔG°
AM1	568.974	538.821	−30.153	273.283	243.757	−29.526
RHF/6-31++G(d,p) non-scaled	614.715	584.020	−30.695	285.266	247.107	−38.159
RHF/6-31++G(d,p) scaled by factor 0.89	531.720	504.917	−26.803	243.250	209.548	−33.702

Table 3
Total energies of optimized structures in kJ/mol. AM1 and PM3 methods were used for packed PANI systems of nine octamers, while HF/6-31G(d) *ab initio* calculations were carried out for a single octamer systems.

Number of dopants	Method	$E_{Bipolaron}$ (kJ/mol)	$E_{Polaron}$ (kJ/mol)	$E_{Polaron} - E_{Bipolaron}$
1	AM1	−8517.3964 ± 0.0037	−8517.5728 ± 0.0029	−0.1764
	PM3	−7751.6263 ± 0.0739	−7751.7707 ± 0.0174	−0.1444
	HF/6-31G(d)	−61968.773 ± 11.102	−61976.861 ± 0.008	−8.088
2	AM1	−8516.5913 ± 0.0070	−8516.8866 ± 0.0093	−0.2953
	PM3	−7754.9350 ± 0.0171	−7755.2237 ± 0.0222	−0.2887
	HF/6-31G(d)	−61767.310 ± 0.061	−61770.147 ± 0.068	−2.837
3	AM1	−8498.5577 ± 0.0082	−8498.9900 ± 0.0179	−0.4323
	PM3	−7742.8746 ± 0.0393	−7743.2058 ± 0.0284	−0.3312
	HF/6-31G(d)	−60757.262 ± 0.013	−60760.839 ± 0.028	−3.577
4	AM1	−8498.0529 ± 0.0078	−8498.6092 ± 0.0187	−0.5563
	PM3	−7746.1636 ± 0.0365	−7746.6612 ± 0.0611	−0.4976
	HF/6-31G(d)	−60706.888 ± 0.014	−60711.046 ± 0.038	−4.158

Table 3 shows the total energies of optimized structures of PANI ES in which 3-methylphenolate ions are inserted. The different configurations by switching the location of hydrogen with that of unshared electron pair orbital on amine group were considered, however the relocation of the hydrogen atoms took place during AM1 and PM3 optimizations. The energy of a polaronic structure is lower than that of the corresponding bipolaronic structure that has same number of atoms, electrons, and dopants. The differences are getting bigger as the number of dopants increases. This result agrees with experiments that the reconstruction of doped structure from bipolaronic to polaronic prefer proceeding in the direction of lowering energy due to Coulomb interaction and so forth [42]. HF/6-31G(d) data in the table are *ab initio* Hartree–Fock calculations with 6-31G(d) basis set for single octamer systems, and also agree with the results from semiempirical calculations for packed PANI cluster of nine octamers.

Table 4 shows that HOMO–LUMO and SOMO–LUMO gaps of *m*-cresol-doped PANI are smaller than those of EB, thus it is found that the acidic dissociation of *m*-cresol can influence the conducting behavior of PANI. Bipolaron energy gap is lower than polaron energy gap and this tendency is consistent with the result predicted in an early study for proton-doped polyemeraldine [25]. Even though SOMO–LUMO gaps from *ab initio* calculations for polaronic structures are slightly higher than those from AM1 and PM3 calculations, it is common that the systems of more atoms show smaller energy gap than those of less atoms. Therefore, HF/6-

Table 4
HOMO–LUMO and SOMO–LUMO levels of optimized structures. AM1 and PM3 methods were used for packed PANI systems of nine octamers, while HF/6-31G(d) *ab initio* calculations were carried out for a single octamer systems.

Number of dopants	Method	Bipolaronic [eV]			Polaronic [eV]		
		HOMO	LUMO	Gap	SOMO	LUMO	Gap
1	AM1	-8.23 ± 0.006	-6.95 ± 0.019	1.28	-6.55 ± 0.011	-3.80 ± 0.011	2.75
	PM3	-8.47 ± 0.033	-7.26 ± 0.094	1.21	-6.66 ± 0.010	-3.54 ± 0.014	3.12
	HF/6-31G(d)	-7.52 ± 0.065	-6.01 ± 0.089	1.51	-5.01 ± 0.006	-0.99 ± 0.013	4.02
2	AM1	-6.08 ± 0.051	-4.90 ± 0.037	1.18	-5.28 ± 0.128	-1.60 ± 0.001	3.68
	PM3	-6.19 ± 0.070	-4.96 ± 0.049	1.23	-5.41 ± 0.105	-1.81 ± 0.008	3.60
	HF/6-31G(d)	-4.64 ± 0.067	-3.38 ± 0.051	1.26	-3.96 ± 0.145	1.12 ± 0.038	5.07
3	AM1	-7.21 ± 0.006	-6.31 ± 0.012	0.90	-6.48 ± 0.120	-3.58 ± 0.068	2.90
	PM3	-7.37 ± 0.022	-6.46 ± 0.024	0.91	-6.55 ± 0.158	-3.83 ± 0.326	2.72
	HF/6-31G(d)	-6.01 ± 0.009	-5.07 ± 0.007	0.94	-5.04 ± 0.134	-0.73 ± 0.061	4.31
4	AM1	-6.09 ± 0.028	-4.93 ± 0.019	1.16	-5.28 ± 0.110	-1.58 ± 0.014	3.70
	PM3	-6.21 ± 0.036	-4.99 ± 0.043	1.22	-5.45 ± 0.101	-1.76 ± 0.016	3.69
	HF/6-31G(d)	-4.63 ± 0.023	-3.42 ± 0.033	1.21	-3.82 ± 0.027	2.69 ± 0.010	6.52

31G(d) results for the doping of single PANI octamer systems are considered to accord with semiempirical calculations.

4. Conclusion

We have carried out computational and experimental studies that are concerned with the acidity of *m*-cresol which is one of the factors enhancing the electron mobility of PANI when CSA is used for dopant. The transport of solvent molecules and of dopant molecules is considered regarding their size and the structure of PANI. It is anticipated that big volume of a CSA molecule restricts the crystallization of PANI and its diffusion into PANI whereas *m*-cresol can diffuse into interstitial positions unless significant disturbance to the crystallization. While the delocalization of π bonds in an undissociated *m*-cresol merely affects the electrical properties of PANI, a 3-methylphenolate ion can decrease energy gap. While MacDiarmid and Epstein found that CSA-doped PANI has still high conductivity after thorough removal of *m*-cresol, we experimentally found that *m*-cresol also works as a dopant in PANI EB.

There are several issues remained for further study. Synergetic protonation of CSA and *m*-cresol needs to be scrutinized more precisely with computational chemistry methods. Polaron separation and local stabilization of bipolarons may depend on the mobilities of CSA and *m*-cresol in PANI because those molecules are more limited to transfer between interstitial position or to rearrange their orientations compared than HCl. Residual *m*-cresol supports PANI maintaining in the form of rigid film, while the elimination of *m*-cresol makes PANI brittle flake. It is also interesting to scrutinize how this macroscopic change is related with its microscopic event or with the electric conductivity of PANI.

Acknowledgement

This work was supported by grant No. KSC-2007-S00-2014 from Korea Institute of Science and Technology Information.

References

[1] Burroughes JH, Bradley DDC, Brown AR, Marks RN, Mackay K, Friend RH, et al. Nature 1990;347:539–41.
[2] Novak P, Muller K, Santhanam KSV, Haas O. Chem Rev 1997;97:207–81.
[3] Ouyang JY, Chu CW, Szmanda CR, Ma LP, Yang Y. Nat Mater 2004;3:918–22.
[4] Joo J, Lee CY. J Appl Phys 2000;88:513–8.
[5] Quadrat O, Stejskal J. J Ind Eng Chem 2006;12:352–61.
[6] Woo DJ, Suh MH, Shin ES, Lee CW, Lee SH. J Colloid Interface Sci 2005;288:71–4.
[7] Choi HJ, Jhon MS. Soft Matter 2009;5:1562–7.
[8] Maity A, Biswas M. J Ind Eng Chem 2006;12:311–51.
[9] Kim JW, Kim SG, Choi HJ, Jhon MS. Macromol Rapid Commun 1999;20:450–2.
[10] Cho MS, Cho YH, Choi HJ, Jhon MS. Langmuir 2003;19:5875–81.
[11] Cao Y, Smith P, Heeger AJ. Synth Met 1992;48:91–7.
[12] Lee SH, Lee DH, Lee K, Lee CW. Adv Funct Mater 2005;15:1495–500.
[13] MacDiarmid AG. Angew Chem Int Ed 2001;40:2581–90.
[14] Epstein AJ, Ginder JM, Zuo F, Bigelow RW, Woo HS, Tanner DB, et al. Synth Met 1987;18:303–9.
[15] Macdiarmid AG, Min Y, Wiesinger JM, Oh EJ, Scherr EM, Epstein AJ. Synth Met 1993;55:753–60.
[16] Lee K, Cho S, Park SH, Heeger AJ, Lee CW, Lee SH. Nature 2006;441:65–8.
[17] Xia YN, Macdiarmid AG, Epstein AJ. Macromolecules 1994;27:7212–4.
[18] MacDiarmid AG, Epstein AJ. Synth Met 1994;65:103–16.
[19] Jayakannan M, Anilkumar P, Sanju A. Eur Polym J 2006;42:2623–31.
[20] Xia YN, Wiesinger JM, Macdiarmid AG, Epstein AJ. Chem Mater 1995;7:443–5.
[21] Kwon O, McKee ML. J Phys Chem B 2000;104:1686–94.
[22] Lee MH, Speyer G, Sankey OF. J Phys Condens Matter 2007;19. Art. No. 215204.
[23] Otto P, Dupuis M. J Chem Phys 1987;86:6309–13.
[24] Boudreaux DS, Chance RR, Wolf JF, Shacklette LW, Bredas JL, Themans B, et al. J Chem Phys 1986;85:4584–90.
[25] Stafstrom S, Bredas JL, Epstein AJ, Woo HS, Tanner DB, Huang WS, et al. Phys Rev Lett 1987;59:1464–7.
[26] Libert J, Bredas JL, Epstein AJ. Phys Rev B 1995;51:5711–24.
[27] Ikkala OT, Pietila LO, Ahjopalo L, Osterholm H, Passiniemi PJ. J Chem Phys 1995;103:9855–64.
[28] Vaschetto ME, Retamal BA, Contreras ML, Zagal JH, Bulhoes LOS. Struct Chem 1995;6:131–40.
[29] Ikkala OT, Pietilac LO, Passiniemi P, Vikki T, Osterholm H, Ahjopalo L, et al. Synth Met 1997;84:55–8.
[30] Lee KH, Song DH, Park BJ, Chin IJ, Choi HJ. Macromol Theory Simul 2009;18, doi:10.1002/mats.200900010.
[31] Choi HJ, Kim TW, Cho MS, Kim SG, Jhon MS. Eur Polym J 1997;33:699–703.
[32] Kim SG, Lim JY, Sung JH, Choi HJ, Seo Y. Polymer 2007;48:6622–31.
[33] Allinger NL, Yuh YH, Lii JH. J Am Chem Soc 1989;111:8551–66.
[34] Schmidt MW, Baldridge KK, Boatz JA, Elbert ST, Gordon MS, Jensen JH, et al. J Comput Chem 1993;14:1347–63.
[35] Jozefowicz ME, Laversanne R, Javadi HHS, Epstein AJ, Pouget JP, Tang X, et al. Phys Rev B 1989;39:12958–61.
[36] Pouget JP, Oblakowski Z, Nogami Y, Albouy PA, Laridjani M, Oh EJ, et al. Synth Met 1994;65:131–40.
[37] Neumann G, Tuijn C. Phys B 2002;315:164–70.
[38] Pouget JP, Jozefowicz ME, Epstein AJ, Tang X, Macdiarmid AG. Macromolecules 1991;24:779–89.
[39] Nakamura J, Ban H, Tanaka A. J Photopolym Sci Technol 1997;10:479–84.
[40] Martell AE, Smith RM. Critical stability constants. New York: Plenum Press; 1977.
[41] Koyama M, Bada K, Sasaki K, Tsuboi H, Endou A, Kubo M, et al. J Phys Chem B 2006;110:17872–7.
[42] Bonnell DA, Angelopoulos M. Synth Met 1989;33:301–10.